Current Research on Biosciences and Biotechnology 8 (1) 2026 18-28

Current Research on Biosciences and Biotechnology

www.crbb-journal.com

FT-IR and GC-MS profiling of *Aurantiochytrium sp.* biomass cultivated on alternative carbon sources in a Wave Junk Fermentor

Suhendra[a*], Bombong Nurpagino[b], Leonny Dwi Rizkita[b], Andri Hutari[c]

[a]Department of Chemical Engineering, Universitas Ahmad Dahlan, Kampus 4 UAD, Jl. Ahmad Yani (Ringroad Selatan) Tamanan Banguntapan Bantul Yogyakarta 55166

[b]Faculty of Medicine, Universitas Ahmad Dahlan, Kampus 4 UAD, Jl. Ahmad Yani (Ringroad Selatan) Tamanan Banguntapan Bantul Yogyakarta 55166

[c]Department of Biology Education, Universitas Muhammadiyah Prof. Dr. HAMKA, Jl. Tanah Merdeka No.20, RT.11/RW.2, Rambutan, Kec. Ciracas, Kota Jakarta Timur, Daerah Khusus Ibukota Jakarta 13830

ABSTRACT

Marine heterotrophic microalgae of the genus *Aurantiochytrium* are a renewable, contaminant-free platform for high-value lipids such as docosahexaenoic acid (DHA) and squalene. This study characterised the dried biomass of an indigenous Indonesian *Aurantiochytrium* sp. isolate, obtained from a Kupang mangrove ecosystem and cultivated in a low-shear, non-impeller Wave Junk Fermentor (registered industrial design IDD000067676). Within a circular-economy framework, the biomass was produced on different carbon sources and screened by high-throughput Fourier-transform infrared (FT-IR) spectroscopy, while its fatty-acid profile was examined by gas chromatography-mass spectrometry (GC-MS). FT-IR spectra of biomass grown on fructose (40 and 50 g/L) were essentially invariant to substrate concentration, whereas raising crude-glycerol concentration from 40 to 50 g/L shifted the O-H stretch from 3345 to 3361 cm^{-1} and produced new bands at 2915 cm^{-1} (aliphatic C-H) and 1043 cm^{-1} (C-O), indicating stimulated de novo lipogenesis. GC-MS of the Glycerol 50 biomass (designated sample NIT1) gave library matches consistent with methyl docosapentaenoate (DPA; C22:5 ω-3) and, more tentatively, DHA (C22:6 ω-3), indicating the presence of long-chain polyunsaturated fatty acids in the lipid fraction. The reported library-match probabilities are identity confidence indices, not concentrations. The biomass FT-IR fingerprint closely resembled that of a premium commercial omega-3/DHA supplement, supporting the commercial potential of this locally sourced biomass as a sustainable feedstock for the pharmaceutical, functional-food and cosmetic sectors.

Article history:

Received 14 Jul 2026
Revised 25 Aug 2026
Accepted 30 Aug 2026
Available online 31 Aug 2026

Keywords:

Aurantiochytrium
docosahexaenoic acid
FT-IR fingerprinting
squalene
Wave Junk Fermentor

*Corresponding authors:
suhendra@che.uad.ac.id

DOI: 10.5614/crbb.2026.8.1/PK8LHSIK

1. Introduction

Global demand for high-value bioactive compounds such as omega-3 fatty acids – particularly docosahexaenoic acid (DHA) – astaxanthin and squalene continues to grow with the expansion of the functional-food, cosmetic and pharmaceutical industries (Furlan et al., 2025; Mariam et al., 2025). DHA is a key functional component for human cognitive and brain development, retinal health and the prevention of cardiovascular and chronic inflammatory disease (Mariam et al., 2025; Swetha and Mathanghi, 2024). Squalene ($C_{30}H_{50}$) is an unsaturated triterpenic hydrocarbon prized by the premium cosmetics industry as an antioxidant, skin-hydration and anti-ageing agent, and is a vital raw material as a vaccine adjuvant in the medical-pharmaceutical sector (Furlan et al., 2025; Suhendra et al., 2022).

To date, the commercial supply of these high-value compounds still relies heavily on the exploitation of conventional marine resources. Squalene is primarily obtained from the liver oil of deep-sea sharks (*Squalus* spp.), driving

the decline of these apex predators and destabilising marine food webs (Furlan et al., 2025; Kwak et al., 2019). Conventional DHA sources derived from captured fish oil face environmental degradation, supply fluctuations from seasonal change, declining global fish stocks from over-exploitation, and the risk of contamination by heavy metals (mercury, arsenic, lead) and microplastics that accumulate in fish adipose tissue (Mariam et al., 2025; Swetha and Mathanghi, 2024).

As a solution, the biotechnological use of marine heterotrophic microorganisms of the family Thraustochytriaceae, especially the genus *Aurantiochytrium*, has emerged as an environmentally friendly, renewable and sustainable alternative production platform (Ganuza et al., 2019; Olsen et al., 2023). *Aurantiochytrium* isolates are fast-growing unicellular oleaginous microalgae able to consume various organic carbon sources under controlled, season-independent conditions (Ganuza et al., 2019; Kwak et al., 2019). They accumulate intracellular lipids as lipid droplets reaching 50-70% of dry cell weight (DCW), rich in saturated fatty acids (particularly palmitic acid, C16:0), squalene and DHA (Mariam et al., 2025; Swetha and Mathanghi, 2024). Furthermore, biomass produced under controlled cultivation is pure, of consistently high quality and entirely free of conventional marine contaminants (Suhendra et al., 2025).

1.1. Indonesian mangrove biodiversity and local isolates

As the archipelagic nation with the world's largest mangrove ecosystem, Indonesia possesses an abundant but systematically under-explored megabiodiversity of marine microbes (Suhendra et al., 2025). Decaying mangrove leaf litter in tropical coastal waters is an ideal natural habitat for saprophytic Thraustochytrids (Suhendra et al., 2022). Despite these outstanding ecological and geographical advantages, internationally reputable research exploiting Indonesian native *Aurantiochytrium* strains remains very limited (Suhendra et al., 2022; 2025). Scientific mastery and legal ownership of native isolates is strategically crucial; registering local strains – such as *Aurantiochytrium* sp. LR52 – in the international National Center for Biotechnology Information (NCBI) database confers national research sovereignty and legal protection against future foreign patent claims or biopiracy (Hutari et al., 2018; Suhendra et al., 2022).

In recent years, exploration of superior indigenous isolates from Indonesian coastal regions has intensified. Through direct plating of mangrove leaf litter from the isolated, high-biodiversity Raja Ampat region (West Papua), an adaptive strain with strong potential for squalene production was isolated (Suhendra et al., 2022). Similar exploration of the coastal ecosystems of Kupang (East Nusa Tenggara) and the mangrove beaches of Yogyakarta has further enriched the national collection of pure *Aurantiochytrium* sp. isolates (Humaidah et al., 2020; Suhendra et al., 2025). These local isolates show robust growth kinetics, adaptability on local waste media, and competitive bioactive-lipid accumulation profiles compared with global reference strains (Humaidah et al., 2020; Suhendra et al., 2025).

1.2. The Wave Junk Fermentor wave-mode bioreactor

Although *Aurantiochytrium* shows very promising bioprocess productivity, large-scale commercial biomass production is often limited by the high operational energy consumption of conventional stirred-tank bioreactors (Mariam et al., 2025; Olsen et al., 2025). Moreover, vegetative *Aurantiochytrium* sp. cells lack a rigid secondary cell wall – they are covered only by a thin organic scale layer – which makes them highly sensitive to the hydrodynamic shear stress generated by rotating mechanical impellers (Kwak et al., 2019; Olsen et al., 2025). Excessive shear can cause mass cell lysis, drastically reducing biocatalyst viability and inhibiting lipid accumulation (Kwak et al., 2019).

To overcome this mechanical constraint, this study employs an innovative, environmentally friendly bioreactor that harnesses wave dynamics: the Wave Junk Fermentor (Industrial Design application A00202300164/IDD000067676, Universitas Ahmad Dahlan) (Universitas Ahmad Dahlan, 2023c). This wave-mode bioreactor is based on a non-impeller rocking-wave kinematic motion (Universitas Ahmad Dahlan, 2023c). The rocking motion generates an internal sloshing wave in the culture medium that ensures nutrient homogeneity and optimal oxygen mass transfer (Olsen et al., 2025; Universitas Ahmad Dahlan, 2023c). The Wave Junk Fermentor markedly reduces mechanical energy input while protecting cellular morphology across three integrated fermentation stages – Standing Culture (SC), Pre-Culture (PC) and Main Culture (MC) – to reach maximum cell density (Olsen et al., 2025; Universitas Ahmad Dahlan, 2023a).

1.3. Alternative carbon sources within a circular economy

From an industrial-economics perspective, the cost of the carbon source – especially refined commercial glucose – is the largest single expense, contributing roughly 30-75% of the total cost of heterotrophic thraustochytrid fermentation (Mariam et al., 2025; Olsen et al., 2025). To improve financial feasibility and upstream sustainability, integrating this cultivation technology into a circular economy through the use of local industrial and agro-industrial waste as an alternative carbon source is highly strategic (Kasim et al., 2025; Suhendra et al., 2025).

Aurantiochytrium has a highly adaptive metabolic flexibility toward non-conventional carbon substrates without significant growth inhibition (Mariam et al., 2025; Suhendra et al., 2025). This versatile behaviour was evaluated comparatively here using different carbon sources: commercial glucose, fructose (Manikan, 2021), crude glycerol from the local biodiesel industry (Mariam et al., 2025; Suhendra et

al., 2025), molasses from sugar refining (Suhendra et al., 2025), and pineapple off-cuts liquid extracts (POCL) from substandard MD2 pineapple (Kasim et al., 2025; Nazir et al., 2020). Fructose- and POCL-rich substrates enhance the expression of key metabolic enzymes such as malic enzyme (ME) and ATP citrate lyase (ACL) that channel carbon flux toward intracellular DHA and squalene biosynthesis (Cui et al., 2019; Nazir et al., 2020). This upstream-downstream optimisation is supported by national patents for a method to produce fatty-acid-rich microalgal biomass (Simple Patent S00202309525) (Universitas Ahmad Dahlan, 2023a) and a squalene purification and fractionation method (Simple Patent S00202313069/ IDS000007427 B) (Universitas Ahmad Dahlan, 2023b).

1.4. FT-IR spectroscopy and comparative benchmarking

To ensure quality and efficiently monitor the chemical composition of the nutrient-rich biomass, a rapid, accurate and non-destructive analytical method is required (Olsen et al., 2023). High-throughput Fourier-transform infrared (FT-IR) spectroscopy was applied as a reliable cellular biochemical screening technology that requires no complex sample preparation or toxic-solvent extraction (Olsen et al., 2023; 2025). The lipid-to-protein (L/P) ratio is calculated directly by comparing the absorbance of the ester carbonyl (-C=O) stretch at 1745 cm^{-1} (a quantitative biomarker of total lipid) with the Amide I band at 1650 cm^{-1} (a biomarker of biomass protein) (Olsen et al., 2023; 2025). Monitoring the L/P ratio provides a real-time picture of the metabolic shift from active growth to functional-lipid accumulation (Olsen et al., 2023).

As a downstream step to validate commercial competitiveness, the functional chemical fingerprint identified by FT-IR was compared directly with premium commercial health supplements marketed as rich in omega-3 (DHA/EPA), astaxanthin and squalene (Furlan et al., 2025; Suhendra et al., 2025). This comparative FT-IR analysis provides crucial scientific evidence of whether biomass from a superior indigenous Indonesian *Aurantiochytrium* strain, produced efficiently via a wave-mode system, delivers bioactive quality equal to or exceeding existing global functional supplements.

The specific novelty of the present study, relative to our recent circular-economy substrate screening in *Aurantiochytrium* (Suhendra et al., 2025), lies in three elements: (i) cultivation in the newly registered, low-shear non-impeller Wave Junk Fermentor (Industrial Design IDD000067676) rather than a conventional stirred-tank system; (ii) direct, non-destructive FT-IR benchmarking of the resulting biomass against premium commercial omega-3/DHA, squalene and astaxanthin supplements; and (iii) characterisation of a distinct indigenous isolate from the Kupang (East Nusa Tenggara) mangrove ecosystem. Whereas Suhendra et al. (2025) focused on comparing industrial-waste carbon sources and their fatty-acid yields, the present work centres on the bioreactor platform and on spectroscopic quality benchmarking of the biomass fingerprint against commercial references.

2. Materials and methods

2.1. Isolate and organism

This study used a pure local marine heterotrophic microalgal isolate of the family Thraustochytriaceae, genus *Aurantiochytrium* sp., obtained from the mangrove ecosystem of Kupang, East Nusa Tenggara (NTT), Indonesia (Universitas Ahmad Dahlan, 2023c). Comparative reference isolates were developed from the mangrove regions of Raja Ampat, West Papua (Suhendra et al., 2022) and Bunaken beach, North Sulawesi (Suhendra et al., 2025), supported by NCBI-registered strain *Aurantiochytrium* sp. LR52 (Hutari et al., 2018). Pure isolates were maintained on Seawater Nutrient Agar (SNA) slants containing 28 g/L nutrient agar and 17.5 g/L artificial sea salt at ~50% (w/w) controlled salinity (Kasim et al., 2025). Stocks were preserved long-term at -80 ° C in cryovials with 50% (v/v) protective glycerol (Olsen et al., 2023).

2.2. Nutrient formulation and cultivation stages

Heterotrophic biomass was produced aseptically through three integrated cultivation stages: Standing Culture (SC), Pre-Culture (PC) and Main Culture (MC) (Suhendra et al., 2025; Universitas Ahmad Dahlan, 2023c). Each stage used a phase-specific medium formulation. (i) *Standing Culture (SC)*: inoculated from a 48h single SNA colony into a 250 mL Erlenmeyer flask with a 20 mL working volume; medium comprised pure commercial anhydrous glucose 0.75 g (37.5 g/L), yeast extract 0.25 g (12.5 g/L) and reef salt 0.36 g (18 g/L), incubated at 30 ° C and 200 rpm for 2 days. (ii) *Pre-Culture (PC)*: 10% of the SC inoculum was transferred aseptically into a 40 mL working volume with glucose 1.5 g (37.5 g/L), yeast extract 0.5 g (12.5 g/L) and reef salt 0.72 g (18 g/L), incubated at 30 ° C and 200 rpm for 2 days. (iii) *Main Culture (MC)*: the PC inoculum was transferred at a 10% (v/v) ratio into the main cultivation vessel and run for 4 days (96 h) in the Wave Junk Fermentor. All nutrient components were sterilised by autoclaving at 120 ° C for 15 min before cultivation (Universitas Ahmad Dahlan, 2023c). The full nutrient composition is given in Table 1.

Table 1. Composition of nutrients across the three cultivation stages (SC, PC and MC).

Component	SC	PC	MC
Carbon source	0.75 g	1.5 g	80 g[a]
Reef salt	0.36 g	0.72 g	7.2 g
Yeast extract	0.25 g	0.5 g	-
MSG	-	-	18 g
Distilled water	50 mL	100 mL	1000 mL

[a]In MC the carbon source was replaced with the test substrate (glucose, fructose, crude glycerol, molasses or POCL) at an initial concentration of ca. 60 g/L.

2.2.1. Variation of carbon source

To evaluate the metabolic flexibility of the local *Aurantiochytrium* sp. within a circular-economy framework, pure glucose in the MC stage was replaced comparatively with several carbon sources at an initial concentration of ca. 60 g/L (Kasim et al., 2025; Suhendra et al., 2025): commercial glucose (positive control); pure fructose (Manikan, 2021); crude glycerol from the local biodiesel industry (Mariam et al., 2025; Suhendra et al., 2025); molasses from the Madukismo sugar mill, Yogyakarta (Suhendra et al., 2025); and pineapple off-cuts liquid extracts (POCL) from rejected MD2 pineapple (Kasim et al., 2025; Nazir et al., 2020). POCL was prepared by mechanically blending rejected pineapple peel and flesh (1:1 w/w) with 50 mL coconut water per 150 g mixture (Suhendra et al., 2025). The mixture was homogenised with a probe sonicator at 25 kHz and 200 W for 10 min, with the amplitude set to 60 μm and 30 s intermittent intervals to keep the temperature below 50 ° C, then finely filtered for use as the main carbon substrate (Suhendra et al., 2025).

2.3. Wave Junk Fermentor operation

The MC stage was carried out in the Wave Junk Fermentor (Industrial Design application A00202300164/ IDD000067676, Universitas Ahmad Dahlan) (Universitas Ahmad Dahlan, 2023c), an innovative non-impeller bioreactor driven by mechanical wave motion. It operates on a rocking-wave kinematic motion mimicking sea-wave hydrodynamics; detachable flexible vessels are mounted on a rocking platform controlled digitally through a control interface (Universitas Ahmad Dahlan, 2023c). The system was set to a maximum rocking angle of 10° , a rocking frequency of 15-25 rpm and gentle aeration (without a rotating impeller) to generate an internal sloshing wave that facilitates nutrient homogenisation and dissolved-oxygen mass transfer without damaging the outer membrane of *Aurantiochytrium* sp. (Olsen et al., 2025; Universitas Ahmad Dahlan, 2023c). MC was conducted at room temperature (28-30 ° C) with the initial medium adjusted to pH 7.0 using 0.1 M NaOH (Kasim et al., 2025). The design and operational components of the bioreactor are shown in Fig. 1.

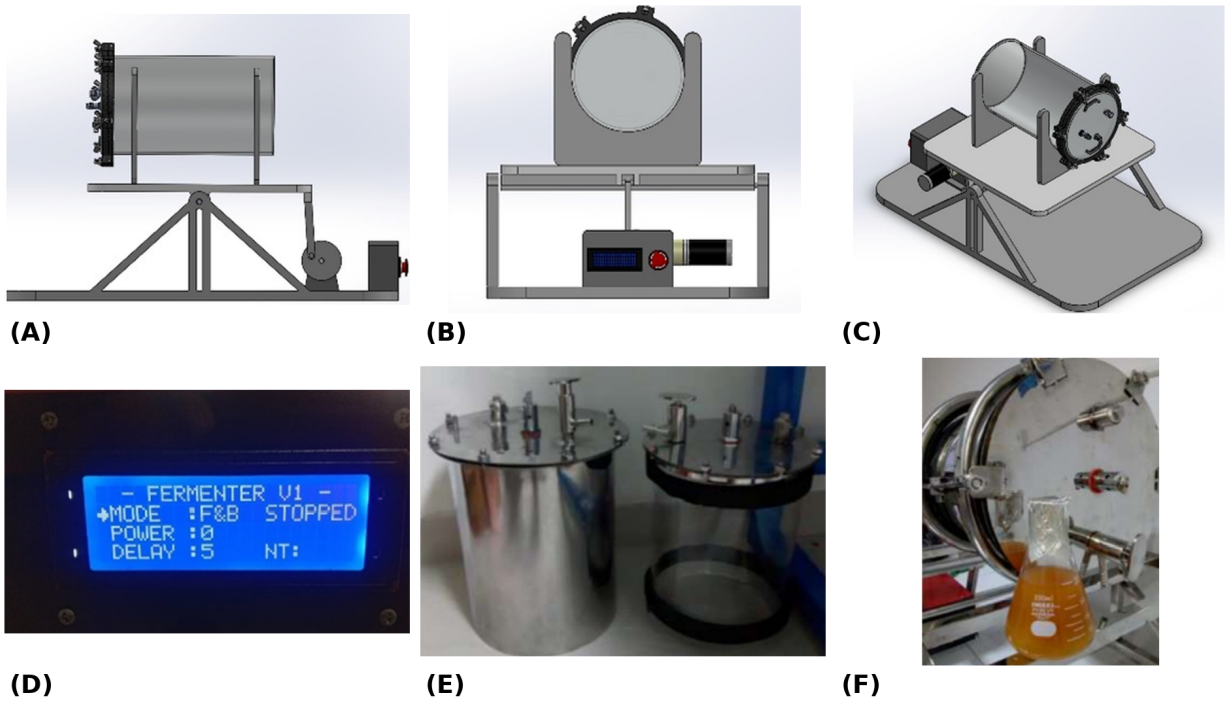

Fig. 1. Design and operational components of the Wave Junk Fermentor used for cultivating *Aurantiochytrium* sp. (A) side view; (B) front view; (C) angled view of the setup; (D) digital control interface for adjusting power, delay and mode; (E) detachable stainless-steel cultivation vessels; (F) the bioreactor in operation, with a culture flask alongside.

2.4. Biomass extraction and squalene purification

After 4 days of MC, wet biomass was separated from the liquid medium by centrifugation at 4000 rpm for 15 min (Suhendra et al., 2022). The wet biomass was washed twice with sterile distilled water to remove residual medium salts, drained through a fine T200 filter cloth and dried in a freeze-dryer at -55 ° C for at least 24 h to a constant dry cell weight (DCW) (Universitas Ahmad Dahlan, 2023b; 2023c).

2.4.1. Squalene-rich fraction separation

Purification of squalene from dried cells followed the registered patent (Simple Patent S00202313069/ IDS000007427 B) (Universitas Ahmad Dahlan, 2023b). (i) *Double-step extraction*: dried biomass was extracted with a

dichloromethane (DCM):methanol mixture (2:1 v/v); the dry-biomass-to-solvent ratio was varied from 10% to 50% (w/v) over three sonication-assisted extraction cycles of 30 min each, with an alternative chloroform:methanol (2:1 v/v) mixture applied under the same parameters (Sulistiawati et al., 2023; Universitas Ahmad Dahlan, 2023b). (ii) *Evaporation*: the combined filtered extract was concentrated on a rotary evaporator (Büchi Rotavapor R-300) at a 51 ° C bath temperature, 80 rpm and 240 mbar to a crude extract (Suhendra et al., 2022; Universitas Ahmad Dahlan, 2023b). (iii) *Silica chromatography*: the crude extract was mixed with silica gel (0.2-0.5 mm particle size) until fully submerged. (iv) *Elution and fractionation*: the silica-extract mixture was eluted with pure n-hexane to bind the non-polar hydrophobic squalene over four cycles; the squalene-rich hexane phase was collected and evaporated to obtain the purified squalene-rich fraction (Universitas Ahmad Dahlan, 2023b). This purification protocol is reported here as an established methodology; the present study does not report a purified-fraction yield or a separate spectrum of the isolated squalene fraction, and the FT-IR squalene-confirmation criterion described in Section 3.5 is therefore presented as an analytical framework for future purification work rather than as a result obtained in this study.

2.5. FT-IR, GC-MS and comparative analysis

2.5.1. FT-IR spectroscopy

Non-destructive cellular biochemical fingerprinting was performed directly on dried biomass using a high-throughput FT-IR system (HTS-FTIR Vertex 70, Bruker Optik, Germany) (Olsen et al., 2023). Twenty milligrams of dried biomass were rehydrated in 500 µL of 0.1% NaCl and homogenised with 250 µm glass beads (Olsen et al., 2025). A 10 µL aliquot of the suspension was deposited on a 384-well IR-transparent silicon microplate and dried at room temperature to a thin film (Olsen et al., 2023). Absorbance spectra were recorded from 4000 to 400 cm^{-1} at 6 cm^{-1} spectral resolution with 64 averaged scans (Olsen et al., 2023). Spectral pre-processing used a second-degree Extended Multiplicative Signal Correction (EMSC) algorithm (Olsen et al., 2025). The lipid-to-protein (L/P) ratio was calculated as the ratio of the ester carbonyl (-C=O) stretch at 1745 cm^{-1} (total-lipid biomarker) to the Amide I band at 1650 cm^{-1} (total-protein biomarker) (Olsen et al., 2023).

2.5.2. Fatty-acid profiling by GC-MS

The detailed fatty-acid methyl ester (FAME) composition was determined by in-situ direct transesterification (Suhendra et al., 2025). Fifty milligrams of dried biomass were placed in a 15 mL acid-resistant reaction vial, to which 500 µL anhydrous methanol and 2 mL of an anhydrous methanol:acetyl chloride mixture (10:1 v/v) were added; the mixture was incubated at 50 ° C for 16 h in a water bath to complete transesterification. The resulting FAME were extracted with 5 mL n-hexane and shaken on a rotary shaker for 15 min to separate the phases; the upper organic phase was collected and the extraction repeated twice (Suhendra et al., 2025). FAME were analysed by GC-MS (Clarus 690 MS coupled to a Clarus SQ8 GC, PerkinElmer) fitted with an Elite-FFAP capillary column (30 m × 0.25 mm, 0.25 µm film) using helium carrier gas (Mariam et al., 2025). Peaks were identified by retention-time matching against the Supelco 37 Component FAME Mix external standard and the NIST spectral library (Mariam et al., 2025; Olsen et al., 2023). The biomass analysed by GC-MS in this study (designated sample NIT1) corresponds to the Main Culture biomass grown on crude glycerol at 50 g/L, i.e. the Glycerol 50 condition described in Section 2.2.1.

2.5.3. Comparison with commercial supplements

The functional quality of the nutrient-rich local biomass was validated by comparing its FT-IR functional-group absorption bands and bioactive components (DHA, squalene, astaxanthin) with three premium global commercial health supplements marketed as rich in astaxanthin, omega-3/DHA and squalene (Furlan et al., 2025; Suhendra et al., 2025). Astaxanthin was included in this comparison solely as an oxygenated-carotenoid reference standard, providing a discriminating FT-IR fingerprint (notably the ionone-ring carbonyl at 1700-1750 cm^{-1} and conjugated C=C bands) for future carotenoid screening; it was not a target bioactive of the present biomass. Each commercial reference supplement was measured in three independent technical replicates (Section 3.3), whereas the biomass FT-IR band positions (Table 2) and GC-MS library-match values (Table 3) are reported as representative single measurements. Because the present study does not report a replicated quantitative variable for the biomass treatments, no inferential statistical test (e.g. one-way ANOVA with a Tukey post-hoc test) was applied to the reported data; comparisons between treatments are therefore made qualitatively on the basis of FT-IR band positions and spectral features.

3. Results and discussion

3.1. FT-IR characterisation of biomass extracts

High-throughput FT-IR spectroscopy was applied to screen and identify the major functional groups constituting the intracellular matrix of the superior local Indonesian *Aurantiochytrium* sp. biomass. Dried biomass harvested from the Wave Junk Fermentor was compared under two carbon substrates – fructose and glycerol – each at two initial concentrations (40 and 50 g/L), giving four comparative conditions: Fructose 40, Fructose 50, Glycerol 40 and Glycerol 50 (Olsen et al., 2025). The corresponding spectra are shown in Fig. 2 and the main band positions are summarised in Table 2.

All biomass samples retained a characteristic cellular biochemical fingerprint, marked by major absorption bands at 3300-3360 cm^{-1} and 1630-1640 cm^{-1}. The broad 3300-3360 cm^{-1} band is associated with the O-H stretching vibration of bound water and carbohydrate in the cell matrix, while the band

near 1630-1640 cm^{-1} represents the H-O-H bending of water and/or the dominant Amide I contribution reflecting structural protein of the microalgal membrane and cytoplasm (Olsen et al., 2025). Because microalgal biomass is a highly complex biological system, each FT-IR band arises from overlapping contributions of similar covalent bonds, so spectral changes must be interpreted comparatively and systematically.

For the fructose treatments, the shift in the main band positions with increasing substrate concentration was minimal. In Fructose 40 the main O-H band appeared at 3338.47 cm^{-1} and the amide/H-O-H band at 1635.06 cm^{-1}; at Fructose 50 these shifted only slightly to 3339.36 cm^{-1} and 1634.46 cm^{-1}. The O-H shift of just 0.89 cm^{-1} and the < 1.0 cm^{-1} amide-region shift indicate that raising fructose from 40 to 50 g/L did not significantly alter the chemical architecture or relative functional-group composition of the biomass, maintaining cellular metabolism in a stable homeostatic state.

In contrast, the glycerol treatments showed a very different spectral response. In Glycerol 40, the O-H band appeared at 3345.32 cm^{-1}, with bands at 2360.30 cm^{-1} and 1639.57 cm^{-1}. When glycerol was raised to 50 g/L, marked spectral changes occurred: the O-H stretch shifted appreciably to a higher wavenumber, 3361.33 cm^{-1} (a shift of 16.01 cm^{-1}), and two representative new bands appeared at 2915.02 cm^{-1} and 1042.91 cm^{-1}.

The band near 2915 cm^{-1} is closely associated with the C-H stretching of aliphatic methylene ($-CH_2-$), a universal biomarker of neutral-lipid (triacylglycerol, TAG) accumulation in intracellular lipid droplets (Olsen et al., 2025). The peak at 1042.91 cm^{-1} lies in the fingerprint region strongly associated with C-O single-bond stretching of lipid esters or structural carbohydrate. The band near 2360 cm^{-1} (2360.30 cm^{-1} in Glycerol 40 and 2360.14 cm^{-1} in Glycerol 50) must be treated with caution; bands in this region are generally influenced by atmospheric CO_2 fluctuations or background noise and were therefore not used as a primary indicator of biochemical change.

Overall, the FT-IR analysis demonstrates that the type and concentration of the carbon source exert markedly different metabolic-regulation effects on the cellular spectral profile of *Aurantiochytrium* sp. Fructose-based biomass showed high compositional stability against substrate-concentration fluctuation, whereas raising glycerol from 40 to 50 g/L triggered a massive upstream metabolic shift – seen as the increased intensity of the aliphatic C-H (2915.02 cm^{-1}) and ester C-O (1042.91 cm^{-1}) bands – indicating more aggressive stimulation of de novo functional-lipid biosynthesis (Olsen et al., 2025).

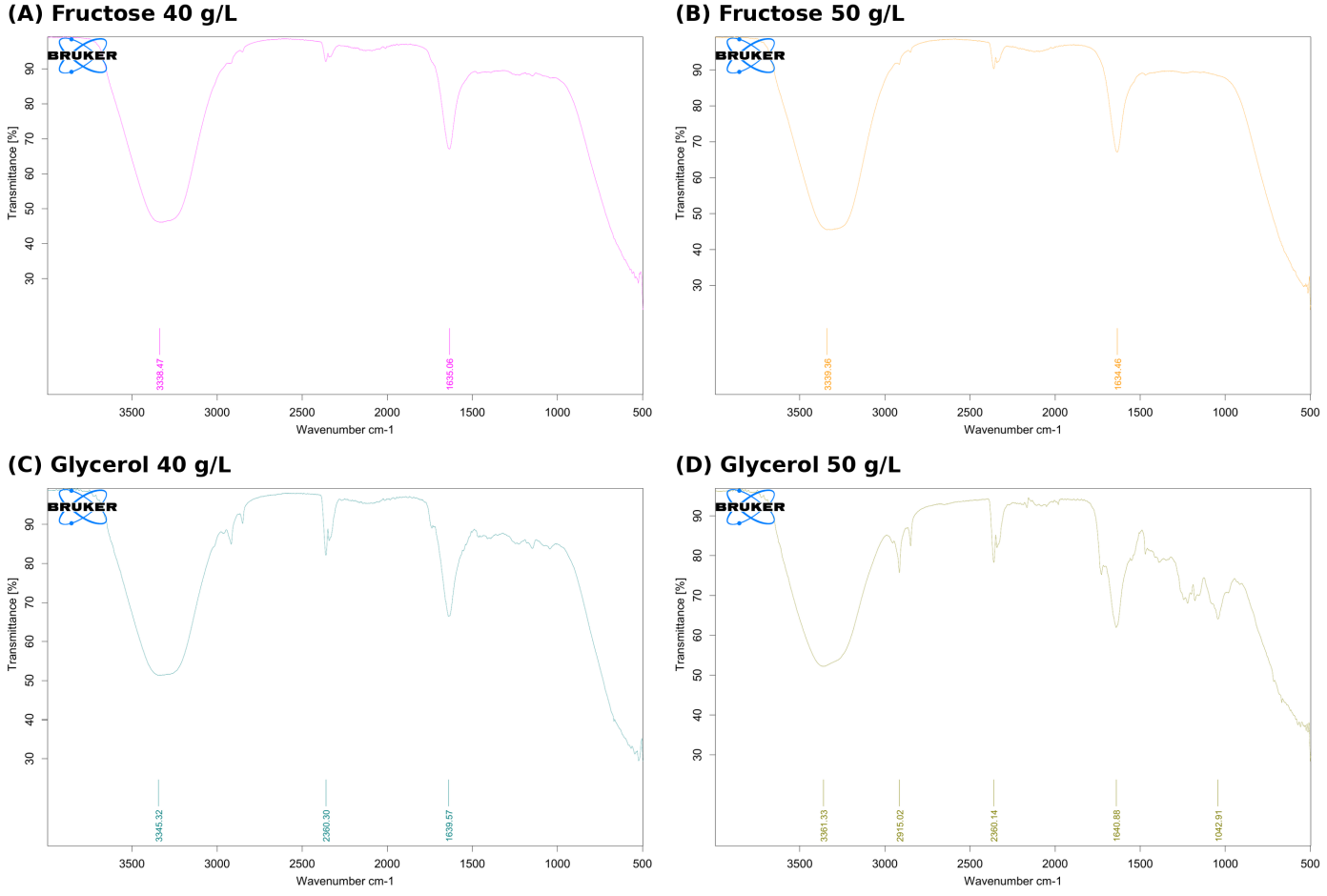

Fig. 2. FT-IR spectra of Aurantiochytrium sp. dried biomass cultivated in the Wave Junk Fermentor on (A) fructose 40 g/L, (B) fructose 50 g/L, (C) glycerol 40 g/L and (D) glycerol 50 g/L. Labelled values are absorption-band positions (cm^{-1}).

Table 2. Main FT-IR absorption bands (cm^{-1}) of *Aurantiochytrium* sp. biomass under the four carbon-source conditions.

Treatment	O-H stretch	C-H aliphatic	CO_2/ background	Amide I / H-O-H	C-O fingerprint
Fructose 40	3338.47	-	-	1635.06	-
Fructose 50	3339.36	-	-	1634.46	-
Glycerol 40	3345.32	-	2360.30	1639.57	-
Glycerol 50	3361.33	2915.02	2360.14	1640.88	1042.91

3.2. Fatty-acid profiling by GC-MS

To validate and specifically identify the long-chain polyunsaturated fatty acids (PUFAs) in the lipid fraction of *Aurantiochytrium* sp. biomass, the GC-MS chromatogram of sample NIT1 – the Main Culture biomass grown on crude glycerol at 50 g/L (Glycerol 50; Section 2.2.1) – was analysed in detail by spectral-library matching (Fig. 3).

The NIT1 chromatogram showed several high-resolution peaks representing fatty-acid methyl ester (FAME) derivatives. NIST library searching gave two essential unsaturated-compound identities (Table 3). Peak 4 was identified as methyl 4,7,10,13,16-docosapentaenoate ($C_{23}H_{36}O_2$; molecular weight 344 g/mol) with a library-matching probability of 31.4%; this is the methyl ester of docosapentaenoic acid (DPA; C22:5 ω-3), a high-value omega-3 fatty acid (Mariam et al., 2025). A further peak gave only a tentative match to docosahexaenoic acid (DHA; C22:6 ω-3; $C_{22}H_{32}O_2$, 328 g/mol), with a low library-matching probability of 7.20%. Because a 7.20% library match is a weak basis for a positive identification, the DHA peak is reported here only as a tentative identification; its confirmation depends on retention-time agreement with the corresponding DHA peak in the Supelco 37 Component FAME Mix external standard (Section 2.5.2), and in the absence of a co-injected pure DHA methyl-ester standard the assignment should be regarded as provisional.

It must be emphasised that the 31.4% (methyl DPA) and 7.20% (DHA) values are library-matching probability indices – the algorithm's identity-confidence against the instrument spectral library – and are not quantitative concentrations. A common error in novice scientific writing is to misread library-matching probability as absolute lipid content. The NIT1 GC-MS result should therefore be reported as a strong qualitative indication of the presence of long-chain PUFAs (omega-3 species such as DPA and DHA) in the *Aurantiochytrium* sp. lipid matrix. Precise quantification requires further analysis with an external calibration curve of pure FAME standards (e.g. the Supelco 37 Component FAME Mix) and optimised column-separation conditions.

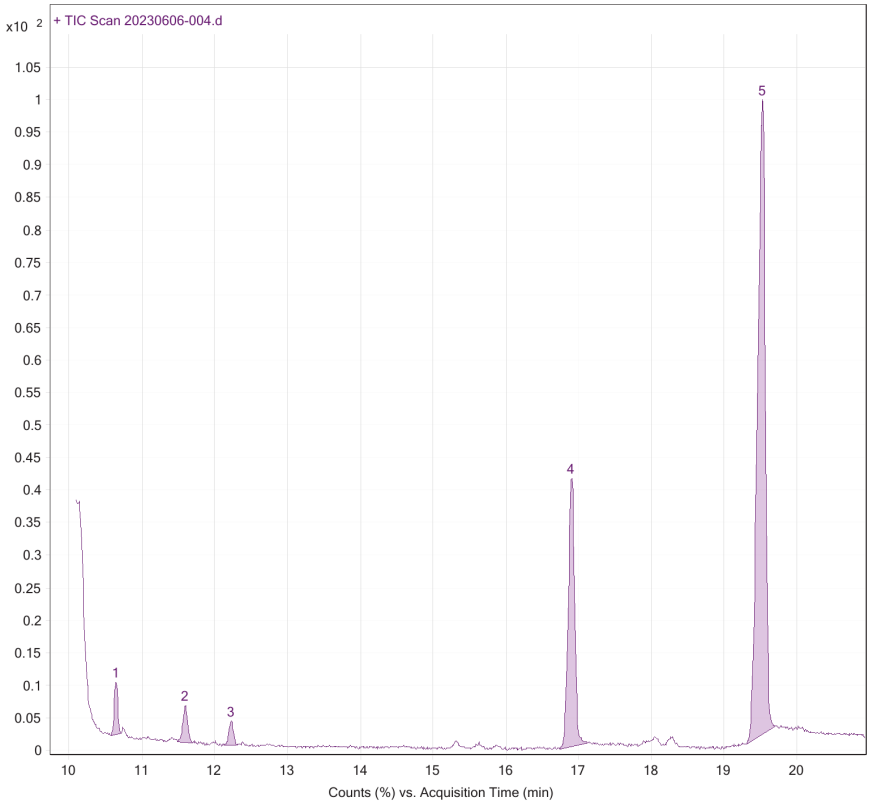

Fig. 3. GC-MS total-ion chromatogram of sample NIT1, showing the major FAME peaks. Peak 4 was identified as methyl docosapentaenoate (DPA).

Table 3. GC-MS library-matching identification of the main unsaturated FAME in sample NIT1.

Peak	Compound	Formula	MW (g/mol)	Library match (%)	Related fatty acid
4	Methyl 4,7,10,13,16-docosapentaenoate	$C_{23}H_{36}O_2$	344	31.4	DPA (C22:5 ω-3)
-	Docosahexaenoic acid (doconexent)	$C_{22}H_{32}O_2$	328	7.20	DHA (C22:6 ω-3)

3.3. FT-IR characterisation of commercial supplements

As a scientific quality benchmark and functional validation reference, FT-IR analysis was performed on three certified premium commercial supplements marketed as rich in astaxanthin, omega-3/DHA and squalene. Each product was measured in three independent technical replicates to ensure reproducible reference fingerprints (Fig. 4).

The three supplement spectra were defined by specific, consistent absorption features. (i) *Astaxanthin* showed the oxygenated unsaturated-hydrocarbon structure typical of carotenoids: a C-H stretching region at 3000-2800 cm^{-1}, a sharp carbonyl (-C=O) peak at 1700-1750 cm^{-1} (from the ketone on the astaxanthin ionone ring) and conjugated C=C contributions at 1600-1650 cm^{-1}. (ii) *Omega-3/DHA* showed a clear long-chain unsaturated fatty-acid profile: dominant sharp aliphatic C-H bands at 2920-2850 cm^{-1} (asymmetric and symmetric -CH_2-), a very strong ester carbonyl band at 1700-1750 cm^{-1} and the characteristic C=C absorption of PUFAs near 1650 cm^{-1}. (iii) *Squalene* was dominated by pure unsaturated-hydrocarbon character: strong aliphatic and unsaturated C-H bands at 3000-2800 cm^{-1}, C=C stretching at 1640-1660 cm^{-1} and -CH_2-/-CH_3 deformation peaks. The most vital distinguishing feature of squalene is the complete absence of a strong carbonyl (-C=O) band at 1700-1750 cm^{-1}, because pure squalene is an oxygen-free, non-oxygenated acyclic unsaturated triterpenoid hydrocarbon.

3.4. Correlation of FT-IR and GC-MS results

Cross-correlating the qualitative FT-IR results with the GC-MS NIT1 data gives a comprehensive, logically complementary picture of the biomass. FT-IR profiles the overall organic functional groups (biochemical profiling), while GC-MS confirms the specific chemical identity of the detected fatty acids. In the Glycerol 50 biomass spectrum, the sharp band at 2915.02 cm^{-1} (aliphatic C-H of the hydrocarbon chain) correlates with the GC-MS detection of long-chain unsaturated fatty-acid esters, namely methyl docosapentaenoate (DPA, Peak 4; 31.4% library match) and, tentatively, DHA (7.20% library match).

This complementary correlation should not be read narrowly as the FT-IR 2915.02 cm^{-1} band being a direct representation of DHA or DPA, because aliphatic C-H vibration is universal to all organic carbon chains (including saturated fatty acids and protein). Nevertheless, the agreement between the increased aliphatic FT-IR intensity and the detection of methyl DPA and DHA in GC-MS provides robust, mutually validating evidence that the Wave Junk Fermentor successfully triggered a metabolic pathway of long-chain omega-3 PUFA-rich lipid accumulation in the harvested cells.

3.5. Comparison of microalgal extract with commercial supplements

The biochemical quality of the *Aurantiochytrium* sp. biomass extract was assessed by comparing its FT-IR spectra with the reference fingerprints of premium commercial supplements, focusing on functional-group similarity and overall spectral resemblance to gauge nutraceutical potential.

The commercial omega-3/DHA spectrum – marked by strong aliphatic C-H, ester carbonyl and unsaturated C=C features – was highly similar to the FT-IR spectrum of the Aurantiochytrium sp. biomass, especially the Glycerol 50 treatment. This is supported by the NIT1 GC-MS data confirming that the main lipid fraction is dominated by omega-3 unsaturated fatty acids (DPA and DHA). The comparison demonstrates that dried biomass from the Wave Junk Fermentor has a functional fatty-acid biochemical profile highly competitive with, and comparable to, commercial omega-3 products in the global functional market (Olsen et al., 2025).

The astaxanthin reference provides valuable comparative information for detecting oxygenated carotenoids. Although no significant carotenoid peak was detected in the *Aurantiochytrium* sp. biomass at this early stage, the astaxanthin reference spectrum will be a very useful screening tool in future optimisation research aimed at inducing secondary antioxidant-pigment synthesis in the local microalga (Humaidah et al., 2020). The squalene reference – defined by the absence of an ester carbonyl peak – provides a clear analytical discriminator between the pure triterpenic hydrocarbon phase and the fatty-acid lipid phase. This is crucial for monitoring the effectiveness and purity of squalene separation by silica-gel adsorption chromatography per registered patent S00202313069; successful purification is confirmed when the FT-IR spectrum of the final hexane-elution fraction shows a complete loss of the carbonyl peak (1700-1750 cm^{-1}) and is dominated by C-H and C=C stretches identical to premium commercial squalene.

3.6. Metabolic plasticity, mechanical aspects and pathways

3.6.1. Carbon-source plasticity and circular economy

The substrate-assimilation flexibility of the local Indonesian *Aurantiochytrium* sp. indicates strong bioprocess potential within a circular-economy framework (Olsen et al.,

2025; Suhendra et al., 2025). Based on the comparative FT-IR analysis, the Glycerol 50 treatment produced more pronounced spectral change and a higher aliphatic-lipid band intensity than the fructose treatments. This agrees closely with Suhendra et al. (2025), who evaluated circular industrial-waste utilisation in a superior local *Aurantiochytrium* sp. and found crude glycerol from biodiesel to be the best substrate, yielding the highest dry cell weight (DCW 53 g) with a very stable biomass emulsion (mean particle size 1874 nm; ultra-homogeneous polydispersity index 0.02677) and the highest DHA methyl-ester content, reaching 54.88% of total fatty acids. Conversely, sugarcane molasses and rejected-fruit waste yielded dominant palmitic acid (methyl hexadecanoate) at 40.87% and 33.89% respectively, with relatively low DHA (0.72% and 4.76%). Crude glycerol is thus the best trigger of DHA-rich TAG accumulation, while molasses and fruit waste favour commercial lipids (palmitic and myristic acids) for the cosmetics industry (Suhendra et al., 2025).

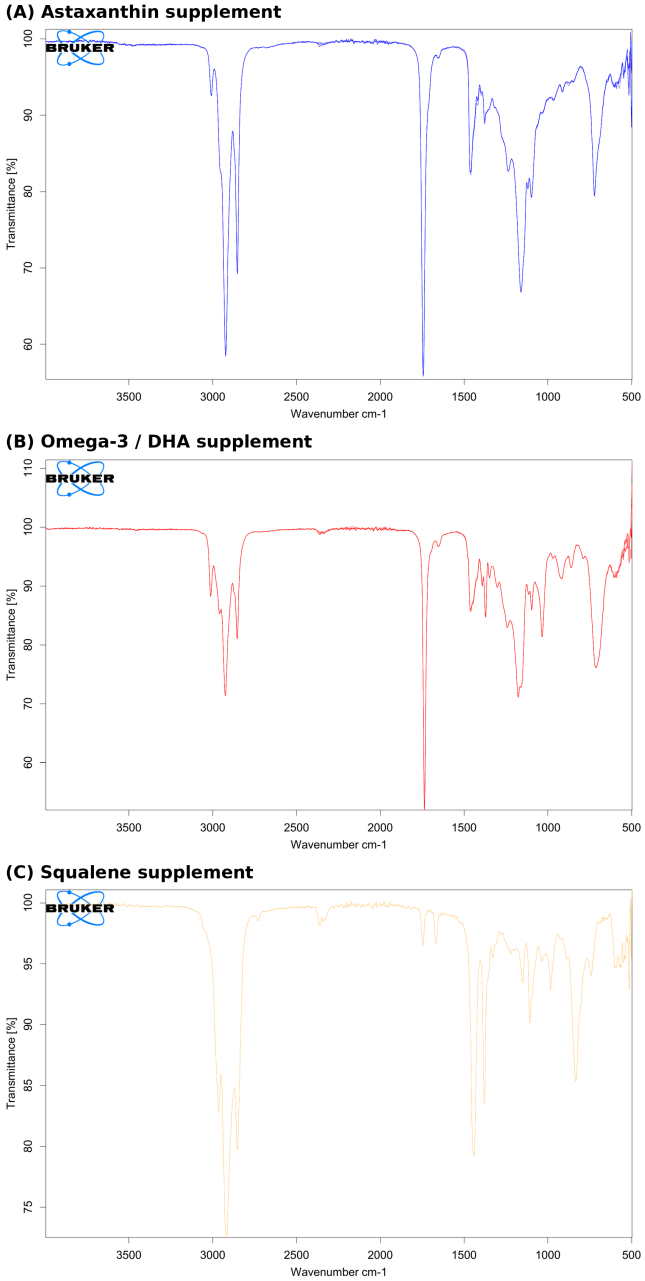

Fig. 4. FT-IR reference fingerprints of premium commercial supplements (three overlaid replicates each): (A) astaxanthin; (B) omega-3/DHA; (C) squalene.

A distinct cellular-assimilation response was also seen with fructose and POCL (Kasim et al., 2025; Manikan, 2021). Manikan et al. (2021) confirmed that Aurantiochytrium sp. SW1 is a rare strain with a preference for fructose over pure glucose, where fructose-based cultivation gave a volumetric DHA accumulation of 3.84 g/L (11% higher than glucose). Biochemically, this advantage arises because fructose enters and is directly converted to fructose-1-phosphate by the membrane phosphoenolpyruvate (PEP)-dependent phosphotransferase system (PTS), bypassing the ATP-consuming

isomerase conversion of glucose to glucose-6-phosphate (Manikan, 2021). This thermodynamic efficiency provides an abundant continuous intracellular carbon flux that feeds the unsaturated-lipid biosynthesis pathway via a polyketide-synthase (PKS)-like system (governed by pfaA, pfaB and pfaC) that operates efficiently under nitrogen-limited conditions (Kasim et al., 2025; Manikan, 2021).

The use of rejected MD2 pineapple off-cuts (POCL) by Kasim et al. (2025) successfully synergised a macro-micronutrient profile in which its fructose (41.70 g/L) and glucose (37.49 g/L) content supported simultaneous co-production of DHA (3.25 g/L) and squalene (60 mg/L) through RSM optimisation. Squalene is synthesised via the shorter cytosolic mevalonate (MVA) pathway from acetyl-CoA, catalysed by the key enzyme squalene synthase (SQS) in an NADPH-dependent reduction (Kasim et al., 2025). The mineral micronutrients (Fe, Mg, Zn) and natural B-complex vitamins in POCL enhanced the expression of key lipid-biosynthesis biocatalysts – malic enzyme (ME), glucose-6-phosphate dehydrogenase (G6PDH) and ATP citrate lyase (ACL) – which together amplify cytosolic NADPH regeneration and accelerate mitochondrial citrate transport for acetyl-CoA formation, increasing functional-lipid accumulation without growth inhibition (Cui et al., 2019; Kasim et al., 2025).

3.6.2. Hydrodynamic advantages of the Wave Junk Fermentor

From a bioprocess-engineering perspective, the robust growth kinetics of the local *Aurantiochytrium* sp. in this reactor are strongly influenced by the mechanical design of the Wave Junk Fermentor (registered Industrial Design IDD000067676) (Universitas Ahmad Dahlan, 2023c). Vegetative Thraustochytrid cells have a smooth outer plasma membrane covered only by a thin, sensitive organic scale that readily lyses under high hydrodynamic shear stress (Kwak et al., 2019). In conventional stirred-tank bioreactors, mechanical impeller rotation – especially at the high speeds needed for oxygen transfer – often damages the microalgal cell membrane, causing mass cell death and drastically lowering functional-lipid accumulation (Kwak et al., 2019; Olsen et al., 2025).

The Wave Junk Fermentor addresses this biophysical challenge through a kinematic rocking-wave system (Universitas Ahmad Dahlan, 2023c). A maximum dynamic tilt angle of 10° and a controlled rocking frequency of 15-25 rpm generate a gentle yet continuous internal sloshing wave (Olsen et al., 2025). This hydrodynamic pattern ensures nutrient homogenisation and an optimal volumetric oxygen mass-transfer coefficient (k_La) without destructive shear (Olsen et al., 2025). A stable oxygen supply across the three fermentation stages (SC, PC, MC) is crucial: stable aerobic conditions early in cultivation support respiratory metabolism for active cell division, while gentle, shear-free mixing maintains maximum biocatalyst viability into the stationary phase for de novo accumulation of omega-3-rich TAG and functional squalene (Kasim et al., 2025; Olsen et al., 2025).

4. Conclusion

This study demonstrates the strong potential of a local Indonesian marine heterotrophic microalga, *Aurantiochytrium* sp., for producing nutrient-rich dried biomass and high-value bioactive compounds. The Wave Junk Fermentor, based on a kinematic rocking-wave motion, protected the shear-sensitive cells while reducing operational energy consumption relative to conventional stirred systems. Within a circular-economy framework the local isolate showed high metabolic plasticity toward alternative carbon substrates from local industrial and agro-industrial waste: (i) crude glycerol from biodiesel was the best substrate for triggering growth and de novo TAG-lipid accumulation, with a DHA methyl-ester content reaching 54.88% of total fatty acids; (ii) rejected MD2 pineapple off-cuts (POCL) supported simultaneous co-production of DHA (3.25 g/L) and squalene (60 mg/L); and (iii) fructose showed higher thermodynamic efficiency than pure glucose via PTS-membrane assimilation, giving a volumetric DHA accumulation of 3.84 g/L.

Non-destructive high-throughput FT-IR spectroscopy proved reliable and precise for rapid screening of intracellular lipid accumulation via the lipid-to-protein (L/P) ratio at 1745 cm^{-1} (ester carbonyl) and 1650 cm^{-1} (Amide I). Comparative FT-IR analysis confirmed that the dried biomass has a spectroscopic fingerprint highly similar to premium global commercial omega-3 supplements, demonstrating the commercial competitiveness and feasibility of the local *Aurantiochytrium* sp. biomass as a superior renewable functional feedstock for the pharmaceutical, functional-food and sustainable-cosmetics sectors.

Acknowledgements

The authors thank Universitas Ahmad Dahlan for research grant support and for access to the registered patents and industrial design underpinning this work (Simple Patents S00202309525 and S00202313069 /IDS000007427 B; Industrial Design A00202300164 / IDD000067676).

Conflict of interest

The authors declare no conflict of interest in this research.

References

Cui G, Wang Z, Hong W, Liu YJ, Chen Z, Cui Q, Song X. 2019. Enhancing tricarboxylate transportation-related NADPH generation to improve biodiesel production by Aurantiochytrium. *Algal Res* 40: 101505. doi: 10.1016/j.algal.2019.101505

Furlan JM, Centenaro GS, Bittencourt Fagundes M, Borges Filho C, Batista I, Bandarra N. 2025. Thraustochytrium sp. and Aurantiochytrium sp.: sustainable alternatives for squalene production. *Mar Drugs* 23(3): 132. doi: 10.3390/md23030132

Ganuza E, Yang S, Amezquita M, Giraldo-Silva A, Andersen RA. 2019. Genomics, biology and phylogeny of Aurantiochytrium acetophilum

sp. nov. (Thraustochytriaceae), including first evidence of sexual reproduction. *Protist* 170(2): 209-32. doi: 10.1016/j.protis.2019.02.004

Humaidah N, Nakai S, Nishijima W, Gotoh T, Furuta M. 2020. Application of Aurantiochytrium sp. L3W for food-processing wastewater treatment in combination with polyunsaturated fatty acids production. *Sci Total Environ* 743: 140735. doi: 10.1016/j.scitotenv.2020.140735

Hutari A, Hidayati W, Mustopa A, Neubauer P. 2018. Aurantiochytrium sp. isolate LR52 small subunit ribosomal RNA gene, partial sequence. Technical report. National Center for Biotechnology Information (NCBI).

Kasim FH, Prabhakaran P, Wan Syaidatul A, Sairi F, Abu Hasan H, Abdul Hamid A, Nazir MYM. 2025. Efficient co-production of docosahexaenoic acid (DHA) and squalene using pineapple off-cuts liquid extracts (POCL) by Aurantiochytrium sp. SW1. *LWT* 229: 118159. doi: 10.1016/j.lwt.2025.118159

Kwak M, Roh S, Yang A, Lee H, Chang YK. 2019. High shear-assisted solvent extraction of lipid from wet biomass of Aurantiochytrium sp. KRS101. *Sep Purif Technol* 227: 115666. doi: 10.1016/j.seppur.2019.06.004

Manikan V. 2021. Two-level factorial analysis of the effect of fructose on DHA biosynthetic capacity of Aurantiochytrium sp. SW1. *Heliyon* 7(2): e06085. doi: 10.1016/j.heliyon.2021.e06085

Mariam I, Rova U, Christakopoulos P, Matsakas L, Patel A. 2025. Tracing diversion of sustainable carbon substrates to docosahexaenoic acid in Aurantiochytrium limacinum: a metabolomics approach. *Chem Eng J* 508: 161147. doi: 10.1016/j.cej.2025.161147

Nazir Y, Halim H, Al-Shorgani NKN, Manikan V, Hamid AA, Song Y. 2020. Efficient conversion of extracts from low-cost, rejected fruits for high-valued docosahexaenoic acid production by Aurantiochytrium sp. SW1. *Algal Res* 50: 101977. doi: 10.1016/j.algal.2020.101977

Olsen PM, Kósa G, Klüver M, Achim K, Shapaval V, Horn SJ. 2023. Production of docosahexaenoic acid from spruce sugars using Aurantiochytrium limacinum. *Bioresour Technol* 376: 128827. doi: 10.1016/j.biortech.2023.128827

Olsen PM, Horn SJ, Byrtusova D, Moen LF, Shapaval V, Hansen LD. 2025. Assessment of different nitrogen sources and bioreactor cultivation strategies during growth of Aurantiochytrium limacinum on spruce sugars. *Algal Res* 86: 103951. doi: 10.1016/j.algal.2025.103951

Suhendra, Septianingsih L, Ariandi TR, Husna M, Laksana ZA, Yuniasih D, Hutari A. 2022. Isolation of Aurantiochytrium microalgae from Raja Ampat and its potential in the vaccine adjuvant raw material industry (in Indonesian). *J Rekayasa Proses* 16(2): 34-44. doi: 10.22146/jrk.72045

Suhendra, Santosa I, Darmawan E, Sunarti, Rangkuti AF, Hutari A. 2025. Circular economy approach to fatty acid production using Aurantiochytrium microalgae and industrial wastes. *Ecol Eng Environ* Technol 26(2): 351-362. doi: 10.12912/27197050/199478

Sulistiawati E, Suhendra, Setyawan M, Mahsunah AH. 2023. Double step method in lipid extraction from biomass Aurantiochytrium sp. powder. Int *J Adv Appl Sci* 12(4): 376-383. doi: 10.11591/ijaas.v12.i4.pp376-383

Swetha N, Mathanghi SK. 2024. Towards sustainable omega-3 fatty acids production – a comprehensive review on extraction methods, oxidative stability and bio-availability enhancement. *Food Chem Adv* 4: 100603. doi: 10.1016/j.focha.2023.100603

Universitas Ahmad Dahlan. 2023a. Metode produksi biomassa mengandung asam lemak bernilai ekonomi menggunakan mikroalga Aurantiochytrium dari hutan bakau Indonesia. Paten Sederhana Indonesia S00202309525, filed 26 September 2023.

Universitas Ahmad Dahlan. 2023b. Metode pemisahan untuk menghasilkan squalene dari mikroalga Aurantiochytrium sp. Paten Sederhana Indonesia S00202313069 / IDS000007427 B, filed 29 November 2023.

Universitas Ahmad Dahlan. 2023c. Perangkat proses fermentasi (Wave Junk Fermentor). Desain Industri Indonesia IDD000067676 / A00202300164, filed 17 January 2023.